PHYSICAL REVIEW B **86**, 081202(R) (2012)

Optical evidence for quantization in transparent amorphous oxide semiconductor superlattice

Katsumi Abe,[1] Kenji Nomura,[2] Toshio Kamiya,[1] and Hideo Hosono[1,2]

[1]*Materials and Structures Laboratory, Tokyo Institute of Technology, 4259 Nagatsuta, Midori-ku, Yokohama 226-8503, Japan*

[2]*Frontier Research Center, Tokyo Institute of Technology, 4259 Nagatsuta, Midori-ku, Yokohama 226-8503, Japan*

(Received 1 July 2012; published 22 August 2012)

We fabricated transparent amorphous oxide semiconductor superlattices composed of In-Ga-Zn-O (*a*-IGZO) well layers and Ga_2O_3 (*a*-Ga_2O_3) barrier layers, and investigated their optical absorption properties to examine energy quantization in the *a*-IGZO well layer. The Tauc gap of *a*-IGZO well layers monotonically increases with decreasing well thickness at $\leqslant$5 nm. The thickness dependence of the Tauc gap is quantitatively explained by a Krönig-Penny model employing a conduction band offset of 1.2 eV between the *a*-IGZO and the *a*-Ga_2O_3, and the effective masses of $0.35m_0$ for the *a*-IGZO well layer and $0.5m_0$ for the *a*-Ga_2O_3 barrier layer, where m_0 is the electron rest mass. This result demonstrates the quantization in the *a*-IGZO well layer. The phase relaxation length of the *a*-IGZO is estimated to be larger than 3.5 nm.

DOI: 10.1103/PhysRevB.86.081202 PACS number(s): 78.66.Jg, 78.67.Pt, 81.05.Gc

Superlattices (SLs) are attractive structures in realizing novel optoelectronic functions that are not attainable with just one constituent material, as demonstrated by, e.g., a quantum cascade laser in III-V semiconductor SLs.[1] It is of interest to examine whether or not the quantization analog of crystalline semiconductors is observable even for amorphous semiconductors. In general, the mean free path of drift carriers in conventional amorphous semiconductors is comparable to the interatomic distances, which leads to physical phenomena different from a good crystalline semiconductor, such as sign anomaly in the Hall voltage.[2,3] A short mean free path also makes it difficult to observe quantum effects because it weakens the interference of wave functions confined in a space larger than the mean free path.

Transparent amorphous oxide semiconductors (TAOSs)[4] are characterized by a strong ionic bonding nature and show unique carrier transport properties. As a consequence, they do not exhibit any sign anomaly in the Hall voltage, and show large Hall electron mobilities of 10–30 $cm^2\ V^{-1}\ s^{-1}$ that are comparable to those in the corresponding crystalline phases. These mobilities provide the mean free paths of 1–3 nm, which are much larger than the interatomic distances. The electron conduction may be understood by a percolation model[5] which is also applied to polycrystalline semiconductors. Combining high electron mobility with other intrinsic advantages of amorphous materials, such as ease in forming thin films at low temperature and high uniformity over wide areas, has been successfully used to obtain high-performance thin-film transistors (TFTs), leading to mass production of amorphous In-Ga-Zn-O (*a*-IGZO) TFTs[6] as backplanes of ultrahigh-resolution flat panel displays.

Here we examine energy quantization in SLs composed of TAOSs.[7] The materials we have chosen are *a*-IGZO, with a Tauc gap of 3.1 eV, as the well layer, and *a*-Ga_2O_3, with a Tauc gap of 4.3 eV, as the barrier layer, the choice being based on the large difference (1.2 eV) in their Tauc gaps. We investigate specifically the thickness dependence of the band gap of *a*-IGZO by the Tauc' method.

Using polycrystalline IGZO (In:Ga:Zn = 1:1:1 in atomic ratio) and polycrystalline β-Ga_2O_3 targets, the respective well and barrier layers were deposited by conventional radio-frequency (rf) magnetron sputtering,[8] at a rf power of 70 W in an Ar-O_2 gas mixture, on SiO_2 glass substrates. The gas flow rates and the total pressures were Ar:O_2 = 19.6:0.4 in sccm and 4 Pa for the *a*-IGZO layers, and Ar:O_2 = 5:5 in sccm and 0.55 Pa for the *a*-Ga_2O_3 layers. The TAOS SLs have structures of a top *a*-Ga_2O_3 barrier/(*a*-IGZO/*a*-Ga_2O_3)$_N$ block (ended by a bottom *a*-Ga_2O_3 barrier)/SiO_2 substrate. All the layers were deposited at room temperature. The SL structure is characterized by the thickness of the *a*-IGZO well layer, L_W, the thickness of the *a*-Ga_2O_3 barrier layer, L_B, and the total number N of well-barrier layers in the stack. A total *a*-IGZO thickness, t_{IGZO} is then given by $L_W \times N$. Two series of SLs were investigated; (i) L_W was varied from 0.9 to 13.3 nm with a fixed t_{IGZO} of 10 or 50 nm, and (ii) L_B was varied from 0.3 to 1.9 nm at L_W = 3.2 nm.

The film thicknesses and the structures of the SLs were estimated from glazing-incidence x-ray reflectivity (GIXR) and high-resolution transmission electron microscopy (HR-TEM). Surface roughness and optical absorption properties of the films were obtained by atomic-force microscopy (AFM) and spectrophotometry, respectively.

The above deposition conditions yielded deposition rates of 1.3 nm/min for the *a*-IGZO and 1.4 nm/min for the *a*-Ga_2O_3 layers. The surface roughness rms values were both $\sim$0.2 nm, guaranteeing a satisfactory layer smoothness to form well-defined thin well and barrier layers. With films 100 nm thick, the fundamental Tauc gaps E_{Tauc} of the *a*-IGZO and the *a*-Ga_2O_3 films were 3.1 and 4.3 eV, respectively. The E_{Tauc} of the *a*-Ga_2O_3 film is much larger than that of the *a*-IGZO film, suggesting that *a*-Ga_2O_3 can be used as a barrier layer against *a*-IGZO as a well layer. The band gap of the crystal phase (β-Ga_2O_3 in the monoclinic system) was reported to be 4.5–4.9 eV due to its strongly anisotropic crystal structure.[9] The E_{Tauc} value of the *a*-Ga_2O_3 film is smaller but would be reasonable.

Figure 1(a) shows GIXR spectra of the SLs with L_W = 0.9, 2.0, 2.8, 4.9, and 7.5 nm for $t_{IGZO} \sim$ 10 nm (the light-blue lines), and with L_W = 1.0 and 3.1 nm for $t_{IGZO} \sim$ 50 nm (the green lines). Employing designed L_W, L_B, and N, the simulation (the red lines) reproduced each of the spectra. Figure 1(b) shows a cross-sectional HR-TEM image of the

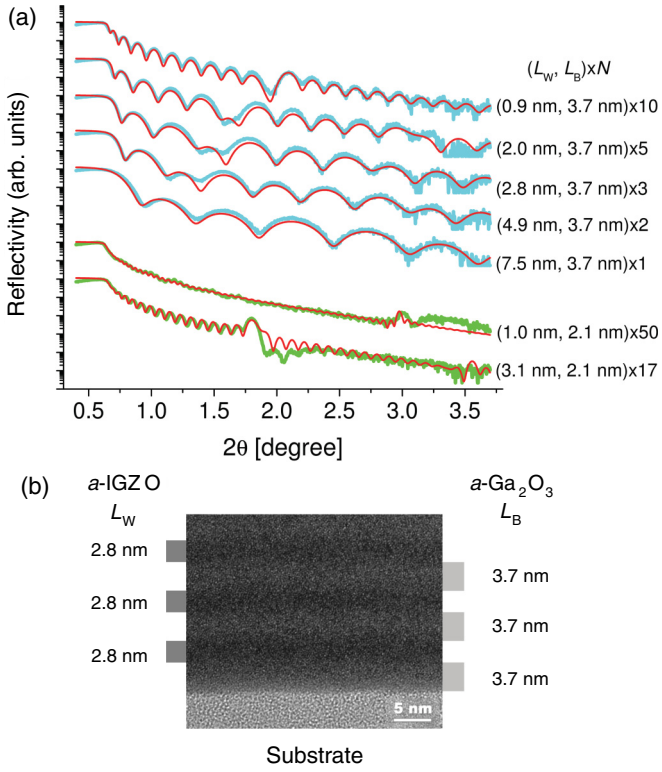

FIG. 1. (Color) (a) Measured and calculated GIXR spectra of the TAOS SLs composed of a-IGZO well and a-Ga_2O_3 barrier layers with various L_W for $t_{IGZO} \sim 10$ or 50 nm (measured spectra: light-blue and green lines; and calculated spectra: red lines). (b) HR-TEM image of the TAOS SL with $L_W = 2.8$ nm and $L_B = 3.7$ nm.

SL with $L_W = 2.8$ nm and $L_B = 3.7$ nm. A stripe pattern is observed with thicknesses that are consistent with the design dimensions L_W and L_B.

Figure 2(a) shows Tauc plots of the SLs with $L_W = 1.0$ and 3.1 nm for $t_{IGZO} \sim 50$ nm, the 100-nm-thick a-IGZO film, and the 100-nm-thick a-Ga_2O_3 film. Because E_{Tauc} of the a-Ga_2O_3 film is 4.3 eV, the optical absorption of the SL for incident photon energies, E, below 4.2 eV is determined mostly by the a-IGZO well layers. E_{Tauc} of the a-IGZO well layer depends therefore on the SL optical absorption for $E < 4.2$ eV. The measured E_{Tauc} of the a-IGZO well layers exhibited blueshifts, as seen in Fig. 2(a) (hereafter, the band gap shift is denoted by ΔE_{Tauc}). Moreover, so as to avoid ambiguity of the Tauc gap in thickness due to the apparent thickness dependence of the Tauc plot slope, the slopes and E_{Tauc} (3.0 and 3.1 eV) of 10- and 50-nm-thick a-IGZO films were used to derive E_{Tauc} and ΔE_{Tauc} of the a-IGZO well layer in the SLs for $t_{IGZO} \sim 10$ and 50 nm, respectively.

Figure 2(b) shows the L_W dependencies of ΔE_{Tauc} for the a-IGZO well layer for $t_{IGZO} \sim 10$ and 50 nm. ΔE_{Tauc} monotonically increases with decreasing L_W at $\leqslant 5$ nm. This result is not affected by t_{IGZO}, indicating that the ΔE_{Tauc} originates in the L_W. Figure 2(c) shows the L_B dependencies of ΔE_{Tauc} for the a-IGZO well layers with $L_W = 3.2$ nm for $N = 5$ and 6. ΔE_{Tauc} exhibits a decrease with decreasing L_B at <1 nm but becomes independent at larger L_B. This result confirms that ΔE_{Tauc} is determined by L_W when L_B is larger than 1 nm.

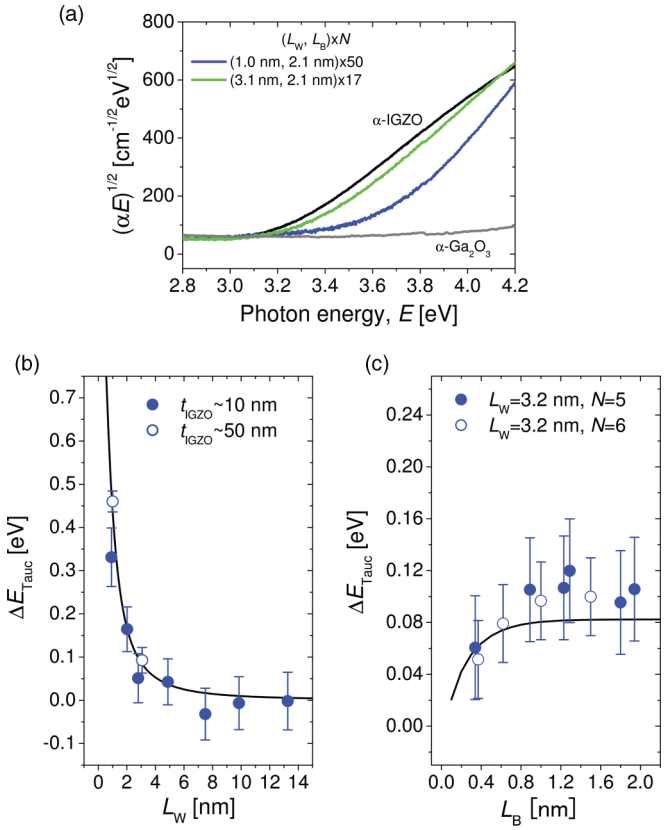

FIG. 2. (Color) (a) Tauc plots of the TAOS SLs with $L_W = 1.0$ and 3.1 nm for $t_{IGZO} \sim 50$ nm (blue and green lines), the a-IGZO film (black line), and the a-Ga_2O_3 film (gray line). (b) The L_W dependence and (c) the L_B dependence of ΔE_{Tauc} of the a-IGZO well layers in the TAOS SLs.

To quantitatively assess these results, we applied the Krönig-Penny (K-P) model, a basic quantum model featuring a periodic rectangular potential. Figure 3 shows the band diagram model incorporating the fundamental band gap values of the a-IGZO and a-Ga_2O_3 thick films. In a preliminary study, we also incorporated the valence band offset, ΔE_V, but we found that the optimum value of ΔE_V would be negligibly small due to the hole's large effective mass (the small dispersion of the valence band[10]). This would be reasonable because the valence bands are mainly formed by

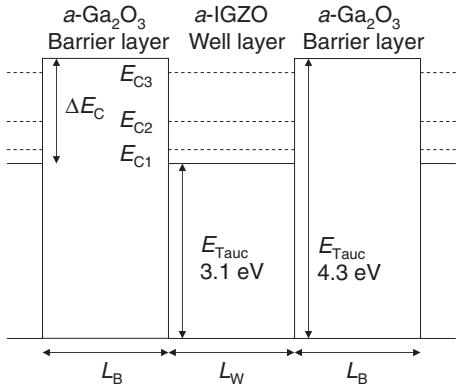

FIG. 3. The proposed energy-band diagram of the TAOS SL.

the oxygen $2p$ orbitals in both the a-IGZO and the a-Ga_2O_3 layers and the energy levels of the valence band edges should be similar. We employed for the electron effective mass of a-IGZO, m_e, a previously reported value of $0.35m_0$,[11] where m_0 is an electron rest mass. For a-Ga_2O_3, the effective mass m'_e of $0.5m_0$ for the crystalline phase[9] was chosen. Based on the K-P model, the energy levels are given by the following equations:

$$\frac{\beta^2-\alpha^2}{2\alpha\beta}\sinh\beta L_B \sin\alpha L_W + \cosh\beta L_B \cos\alpha L_W = \cos k(L_W + L_B), \quad (1)$$

where α and β are defined as

$$\alpha = \sqrt{\frac{2m_e E_{Cn}}{\hbar^2}} \quad (2)$$

and

$$\beta = \sqrt{\frac{2m'_e(\Delta E_C - E_{Cn})}{\hbar^2}}, \quad (3)$$

with k the wave vector projected along the stacking direction of the SL, $\hbar$ the Planck constant, E_{Cn} the nth quantized energy level from the conduction band edge, and ΔE_C the conduction band offset between the a-IGZO and the a-Ga_2O_3 (Fig. 3). The observed ΔE_{Tauc} corresponds to the minimal E_{Cn}, i.e., E_{C1} at $k = 0$. The solid line in Fig. 2(b) shows the calculated result using the designed L_W, L_B, and the band diagram in Fig. 3. The result exhibits fairly good agreement with this simple model, and substantiates the claim that the blueshift in E_{Tauc} originates from quantum confinement in the a-IGZO wells.

The calculated L_B dependence of ΔE_{Tauc} [the solid line in Fig. 2(c)] also shows satisfactory agreement lying within data point errors, and reproduces the decrease in ΔE_{Tauc} at $L_B < 1$ nm. This result supports the selection of $m'_e = 0.5m_0$ for a-Ga_2O_3. It further implies that the electron effective mass of a-Ga_2O_3 is similar to that of the crystalline phase, which is observed for ionic amorphous oxides including a-IGZO.[11]

The SL composed of a crystalline well material shows a clear step structure in the optical absorption spectrum. On the other hand, steplike absorption spectra were not observed for amorphous Si SLs,[12] because of the relaxation of the k-selection rule in the optical transition of amorphous materials.[13,14] So, we consider it reasonable that the step structure is not clear also in the TAOS SLs.

The quantization behavior in Fig. 2(b) provides a rough estimation of a phase relaxation length for electrons in a-IGZO. The phase relaxation time and length represents the time and length in which a wave function maintains its phase information, thereby it can interfere with other wave functions and itself, respectively.

Here we consider the phase relaxation is caused by the amorphous structure of a-IGZO, and the phase relaxation time τ_e is given by $L_{\tau e}/v_e$, where $L_{\tau e}$ is the phase relaxation length for electrons, and v_e is the velocity of the electrons and is estimated to be $v_e = \sqrt{2E_{C1}/m_e}$ for the lowest quantized level with energy E_{C1}. On the one hand, from the energy-time uncertainly relation, τ_e causes uncertainty in energy $\delta E_{C1} \sim \hbar/\tau_e$. On the other hand, the band edge energy of bulk a-IGZO (E_C) is not affected by the energy uncertainty because v_e approaches zero, τ_e diverges, and consequently δE_C tends to zero. Therefore, $L_{\tau e}$ should satisfy $E_{C1} > \delta E_{C1}$ to observe the band edge shift originating from the quantization, which gives rise to

$$L_{\tau e} = v_e\tau_e > \sqrt{\frac{2\hbar^2}{m_e E_{C1}}}. \quad (4)$$

Using the band diagram in Fig. 3 in the K-P model, $L_W = 5$ nm yields $E_{C1} \sim 35$ meV. Equation (4) then indicates that $L_{\tau e} > 3.5$ nm.

In carrier transport phenomena, different transport phenomena are governed by different relaxation times and lengths originating from different scattering mechanisms; e.g., drift mobility is expressed by momentum relaxation time and drift-carrier mean free path. The momentum relaxation time and the drift-carrier mean free path are affected by all kinds of scattering effects, but some of them can take place without losing the phase information of the electron wave function (e.g., alloy scattering). Therefore, the phase relaxation time and length are close to or longer than the momentum relaxation time and the drift-carrier mean free path, respectively. This is supported by the data of other materials; e.g., the phase relaxation lengths of crystalline Si and GaAs, whose mobilities are higher than 1000 $cm^2\ V^{-1}\ s^{-1}$, are between tens and hundreds nm, and close to or a little longer than their mean free paths.[15] On the other hand, polycrystalline metals, whose mobilities are tens $cm^2\ V^{-1}\ s^{-1}$, have a phase relaxation length of several μm, and it is much longer than the mean free path of tens nm.[16] For a-IGZO, the electron transport is governed by percolation conduction and alloy scattering that are caused by the disordered structure[5,11] and not by photon scattering, unlike Si and GaAs. These considerations explain the conclusion that the phase relaxation length of a-IGZO is longer than the drift-carrier mean free path of $\sim$1 nm.[5]

An interesting note is that using an optical method energy quantization was reported also in a hydrogenated amorphous silicon (a-Si:H) SL.[12,17] a-Si:H shows a Hall sign anomaly[2] and its electron mobility is low ($<1\ cm^2\ V^{-1}\ s^{-1}$). However, electron mobility at a high-energy extended state is estimated by several methods to be $\sim 10\ cm^2\ V^{-1}\ s^{-1}$,[18–20] which is expected to be observed if high-density electron doping is possible and the Fermi energy is raised to above the mobility edge. The a-Si:H SL[17] showed that the observed ΔE_{Tauc} at $L_W = 5$ nm and the estimated m_e were 30 meV and $0.6m_0$, respectively. It is thus realistic to consider that the phase relaxation length and drift-carrier mean free path of a-Si:H are not so different from those of the a-IGZO. Notwithstanding that the chemical bonding nature of a-Si:H (covalent bonding) and TAOS (ionic bonding) are completely different, distinct optical quantization effects are observed in both systems. This finding implies that energy quantization occurs in a SL composed of a wide variety of amorphous semiconductors as long as the well thickness is comparable to the phase relaxation length.

This work was supported by Funding Program for World-Leading Innovative R&D on Science and Technology, FIRST Program, through Japan Society for Promotion of Science and Element Strategy for Science and Technology Program, MEXT.

[1]J. Faist, F. Capasso, D. L. Sivco, C. Sirtori, A. L. Hutchinson, and A. Y. Cho, Science **264**, 553 (1994).
[2]P. G. Le Comber, D. I. Jones, and W. E. Spear, Philos. Mag. **35**, 1173 (1977).
[3]E. Mytilineou and M. Roilos, Philos. Mag. B **37**, 387 (1978).
[4]H. Hosono, M. Yasukawa, and H. Kawazoe, J. Non-Cryst. Solids **203**, 304 (1996).
[5]T. Kamiya, K. Nomura, and H. Hosono, Appl. Phys. Lett. **96**, 122103 (2010).
[6]K. Nomura, H. Ohta, A. Takagi, T. Kamiya, M. Hirano, and H. Hosono, Nature (London) **432**, 488 (2004).
[7]H. Ohta, R. Huang, and Y. Ikuhara, Phys. Status Solidi (RRL) **2**, 105 (2008).
[8]H. Yabuta, M. Sano, K. Abe, T. Aiba, T. Den, H. Kumomi, K. Nomura, T. Kamiya, and H. Hosono, Appl. Phys. Lett. **89**, 112123 (2006).
[9]N. Ueda, H. Hosono, R. Waseda, and H. Kawazoe, Appl. Phys. Lett. **71**, 933 (1997).
[10]T. Kamiya, K. Nomura, and H. Hosono, Phys. Status Solidi A **206**, 860 (2009).
[11]A. Takagi, K. Nomura, H. Ohta, H. Yanagi, T. Kamiya, M. Hirano, and H. Hosono, Thin Solid Films **486**, 38 (2005).
[12]B. Abeles and T. Tiedje, Phys. Rev. Lett. **51**, 2003 (1983).
[13]K. Hattori, T. Mori, H. Okamoto, and Y. Hamakawa, Phys. Rev. Lett. **60**, 825 (1988).
[14]K. Hattori, H. Okamoto, and Y. Hayakawa, J. Non-Cryst. Solids **114**, 687 (1989).
[15]C. W. J. Beenakker and H. van Houten, Solid State Phys. **44**, 1 (1991).
[16]S. Washburn and R. A. Webb, Adv. Phys. **35**, 375 (1986).
[17]H. Hirose and S. Miyazaki, Trans. Electron Devices **36**, 2873 (1989).
[18]P. G. Le Comber and W. E. Spear, Phys. Rev. Lett. **25**, 509 (1970).
[19]R. A. Street, J. Kakalios, and M. Hack, Phys. Rev. B **38**, 5603 (1988).
[20]T. Leroux and A. Chenevas-Paule, J. Non-Cryst. Solids **77-78**, 443 (1985).